Cellular Signalling 64 (2019) 109410

Contents lists available at ScienceDirect

Cellular Signalling

journal homepage: www.elsevier.com/locate/cellsig

Butyrate mediated regulation of RNA binding proteins in the post-transcriptional regulation of inflammatory gene expression

Aydan Torun[a,1], Shabnam Enayat[a,1], Ilir Sheraj[a], Sinem Tunçer[a,2], Doğukan Hazar Ülgen[a,3], Sreeparna Banerjee[a,b,*]

[a] Department of Biological Sciences, Orta Dogu Teknik Universitesi (ODTU/METU), Ankara 06800, Turkey
[b] Cancer Systems Biology Laboratory (CanSyl), Orta Dogu Teknik Universitesi (ODTU/METU), Ankara 06800, Turkey

ARTICLE INFO

Keywords:
Butyrate
Post transcriptional regulation
HuR
COX-2
Inflammation

ABSTRACT

Short chain fatty acids (SCFAs) are produced by commensal bacteria in the gut and are known to reduce inflammation through transcriptional inhibition of cytokines and inflammatory proteins such as cyclooxygenase-2 (COX-2). Butyrate is a SCFA that was reported to alter the mRNA stability of inflammatory genes by increasiing the expression of the RNA binding protein (RBP) Tristetraprolin (TTP). We have hypothesized that butyrate may regulate gene expression post-transcriptionally through global effects on the expression or cytoplasmic translocation of RBPs. Using bioinformatics analyses of publicly available microarray data as well as colon cancer cell lines treated with sodium butyrate, we have observed that butyrate treatment led to a general reduction in expression of several (but not all) RBPs and inhibition in the cytosolic translocation of HuR, a well-known stabilizing RBP. This was reflected in reduced NanoLuc reporter activity of several different AU-rich element (ARE) sequences in the presence of butyrate; this suppression was retained even when HuR was overexpressed. Mechanistically, we have shown that reduced activity of HuR was related to decreased phosphorylation of p38 and MK2 and enhanced phosphorylation of Chk2. As a proof of concept, we show butyrate-mediated inhibition in binding of HuR to the 3'UTR of COX-2 mRNA resulting in reduced mRNA and protein levels of the inflammatory gene. Overall, our data suggest that butyrate can reduce the expression of inflammatory genes not only by transcriptional regulation, but also by post-transcriptional regulation via inhibition of mRNA stabilizing proteins.

1. Introduction

Butyric acid is a short chain fatty acid (SCFA) that is generated in the gut along with acetic acid and propionic acid when bacterial species such as those belonging to the class *Clostridia* clusters IV and XIVa metabolize resistant starches and fibers in the diet [1,2]. Butyrate plays several important roles in the human colonic epithelial cells including energy generation, maintenance of the gut barrier, as well as immunomodulatory and anti-inflammatory functions [1]. It has been well-documented that butyrate can reduce proliferation and induce apoptosis and differentiation of transformed colonic epithelial cells [3]. Moreover, colorectal cancer (CRC) patients have reduced representation of butyrate producing bacteria in fecal samples compared to healthy individuals [4]. Several butyrate mediated effects can be attributed to its epigenetic histone deacetylase inhibition (HDACi) activity, leading to the de-repression of genes such as the cyclin dependent kinase inhibitor p21, the proapoptotic protein Bcl-2 homologous antagonist/killer (BAK) or the orphan nuclear receptor PPARγ [5].

Butyrate has been recognized in the colon for reducing inflammation primarily through the suppression of nuclear factor kappa B (NF-κB) [3,6]. In fact, butyrate has been used in clinical trials with some success in patients with inflammatory bowel disease and Crohn's disease [7]. In a recent trial, obese patients subjected to oral supplementation of sodium butyrate for 4 weeks did not show any major changes in the cytokine profile in their peripheral blood mononuclear cells (PBMCs) indicating that local rather than systemic changes may be

* Corresponding author at: Department of Biological Sciences, Orta Dogu Teknik Universitesi (ODTU/METU), Ankara 06800, Turkey.
E-mail address: banerjee@metu.edu.tr (S. Banerjee).
[1] Equal contribution.
[2] Present address: Vocational School of Health Services, Department of Medical Laboratory Techniques, and Biotechnology Application and Research Center, Bilecik Şeyh Edebali University, Bilecik, 11,230, Turkey.
[3] Present address: Department of Biochemistry, University of Oxford, South Parks Road, Oxford OX1 3QU, United Kingdom.

https://doi.org/10.1016/j.cellsig.2019.109410
Received 31 May 2019; Received in revised form 28 August 2019; Accepted 31 August 2019
Available online 02 September 2019
0898-6568/

expected from butyrate supplementation [8].

During an inflammatory response, cytokine secretion is rapidly stimulated through increased activity of a number of transcription factors. Once the purpose of the inflammatory response has been met, cytokine secretion needs to revert to homeostatic levels in order to promote resolution of inflammation. Many studies have indicated that RNA binding proteins (RBPs) can bind to *cis*-elements such as Adenylate- and Uridylate-rich elements (ARE) present in the 3′ untranslated regions (3' UTRs) of inflammatory mRNAs to rapidly regulate their levels and thereby adapt to changing environmental conditions [9,10]. Some of these proteins promote mRNA stabilization thereby leading to increased protein expression, e.g. hnRNP A1 and HuR/ELAVL1, whereas others primarily decrease mRNA expression through destabilization, e.g. AUF1 (hnRNP D), tristetraprolin (TTP), TIAR and TIA-1, and CUGBP2 [11]. Recognition of AREs by destabilizing RBPs can lead to a decay of mRNAs through deadenylation of the mRNA [12], decapping or a delay in translation [13]. Stabilizing RBPs, on the other hand, function by preventing the association of destabilizing RBPs or miRNAs that repress translation [14]. Competition between these stabilizing and destabilizing RBPs for binding to similar sequences at the 3'UTR may decide the final fate of the mRNA [15].

RBPs are believed to be functional mostly in the cytoplasm by sequestering target mRNAs in processing bodies. The localization of these proteins in the nucleus or the cytoplasm is closely regulated [15,16]. For example, signaling through the checkpoint protein Chk2 enhances the translocation of HuR to the cytoplasm to enhance the half-life of target mRNAs, while in the nucleus it can participate in the regulation of pre-mRNA splicing [17].

A few studies in the literature have suggested the intriguing idea that butyrate, in addition to epigenetically regulating gene expression through its HDACi activity, may also post-transcriptionally regulate the expression of various genes via the regulation of expression of RBPs. Thus, Tristetraprolin (TTP) also known as zinc finger protein 36 (ZPF36), a destabilizing RBP, was shown to be transcriptionally upregulated in the presence of butyrate, leading to a reduction in the transcript levels of the inflammatory protein COX-2 [18] and the cell cycle protein cyclin B1 [19]. Butyrate was also shown to reduce the mRNA levels of TNFα through an upregulation of the RBP TIS11B [20], member of a family of proteins that also includes TTP. The 3'UTR of COX-2 has a length of approximately 2 kilobases and was classified as a Cluster 3 ARE with a stretch of WAUUUAUUUAUUUAW [21] that are mostly located in the first 100 or so bases and respond to the presence of various regulatory proteins, including RBPs [22].

In this study we have hypothesized that butyrate may affect the global expression of RBPs. Mining publicly available microarray data (GSE45220 [23], GSE4410 [24] and GSE17397 [25]) we observed that there was an overall suppression of RBP expression in butyrate treated colon epithelial cells and examined mechanistically whether butyrate mediated suppression of RBPs could affect the post-transcriptional regulation of genes. Using a number of different colon cancer cell lines, we confirmed that butyrate reduced the expression and/or cytoplasmic translocation of several different RBPs as well as their binding to different ARE sequences. Focusing on HuR, a stabilizing RBP, we show that the reduction in cytoplasmic levels of the protein could be attributed to an increase in the phosphorylation of the checkpoint protein Chk2 and a reduction in the phosphorylation of the stress activated p38 and MAPKAPK2 (MK2) pathway. Finally, as a proof of concept, we examined the regulation of expression of COX-2 in the presence of butyrate. We observed a dose dependent decrease in the expression of COX-2 in cells treated with butyrate. Interestingly, this reduction was not through an inhibition of the inflammatory transcription factor NF-κB, but a decrease in the binding of HuR to the 3'UTR of COX-2 [26]. Overall, our data show that butyrate, in addition to its well-known epigenetic role of inhibiting histone deacetylases, may also regulate gene expression at the post-transcriptional level by modulating the activity of RBPs.

2. Materials and methods

2.1. Bioinformatics analyses

Three publicly available microarray datasets were analyzed for this study. The first dataset, GSE45220 [23], consisted of expression values for HT-29 cells treated with vehicle (control) or 2 mM sodium butyrate (NaBt) for 24 h. The second dataset, GSE17397 [25], consisted of expression values for HeLa cells treated with vehicle (control) or 5 mM sodium butyrate (NaBt) for 15 h. The third dataset, GSE4410 [24], consisted of expression values for a non-transformed mouse colonic epithelial MCE301 cell line treated with vehicle (control) or 2 mM NaBt for 6-, 12- and 24 h.

The raw data for GSE45220 and GSE17397 were downloaded from the GEO Database (https://www.ncbi.nlm.nih.gov/geo/) and normalized by Robust Multichip Average (RMA) [27] and *oligo* [28] packages. A total of 414 human RBPs were downloaded from the RBPDB database [29] and matched to the probes by their ENSMBL IDs and Gene Symbols. Finally, a total of 446 probes representing 395 unique human RBPs were extracted from the expression matrix. Probe annotations were carried using the gene-centric *hugene10sttranscriptcluster.db* [30] and *huex10sttranscriptcluster.db* [31] packages, respectively. Differential expression was determined using *limma* package from Bioconductor [32]. All data normalization and annotations were carried out in the R environment 3.6.0 version for Windows.

For GSE4410, the pre-normalized microarray data was downloaded from Array Express database (https://www.ebi.ac.uk/arrayexpress/experiments/E-GEOD-4410/?query=gse4410) and transformed in logarithmic scale of base 2. A total of 404 mouse RBPs were downloaded from the RBPDB database [29]. The annotation file for Affymetrix Mouse Expression 430A Array release number 35 was downloaded from the Affymetrix webpage (http://www.affymetrix.com/support/technical/byproduct.affx?product=moe430). Affymetrix probes that quantify the expression of the mouse RBPs were extracted from the annotation file in R language environment version 3.5.1 by using the relevant functions of *dplyr* package (https://cran.r-project.org/web/packages/dplyr/index.html). In total, 608 probes representing 301 unique genes were matched and used for further analysis. After differential expression (DE) analysis, in the cases of genes with two or more probes, only the most significant ones were used. Separate DE analysis was carried out for control versus each treatment time point (6, 12 and 24 h) using the *limma* package from Bioconductor [32], and it showed no overall significant gene (FDR < 0.1) due to the low number of replicates (2 per case). Therefore, our selection criterion was based on $p < 0.05$.

Interaction scores for the networks were downloaded and transferred to Cytoscape version 3.7.1 for visualization [33]. Heat maps were generated using the Morpheus software of Broad Institute (https://software.broadinstitute.org/morpheus).

2.2. Cell culture and treatments

Caco-2 and HT-29 cells were purchased from ŞAP Enstitüsü (Ankara, Turkey), HCT-116 cells were purchased from the German Cancer Research Center (DKFZ, Heidelberg, Germany). Caco-2 cells were grown in Eagle's Minimum Essential Medium (EMEM) (Thermo Fisher Scientific, Boston, MA, USA) containing 20% FBS, 2 mM L-glutamine, 1× non-essential amino acids, 1% penicillin-streptomycin and 1 mM sodium pyruvate. HT-29 and HCT-116 cells were cultured in McCoy's 5A modified medium supplemented with 10% FBS, 2 mM L-glutamine and 1% penicillin–streptomycin. Cells were grown at 37 °C in a humidified atmosphere of 5% CO_2/95% air. Unless otherwise indicated, all cell culture media and components were purchased from Biological Industries (Beit Haemek, Israel). All cells were routinely tested for mycoplasma contamination [34] and cultured with a prophylactic dose (2.5 μg/ml) of Plasmocin® (Invivogen, Toulouse,

France). Where indicated, cells were treated with sodium butyrate (NaBt, Sigma Aldrich Chemie GmbH, Taufkirchen, Germany) at a concentration of 1, 3 or 5 mM for 6 h or 48 h. Water was used as vehicle (annotated as veh. in figures) for NaBt. For the actinomycin D (ActD, Sigma) chase assay, HT-29 cells were treated with NaBt (5 mM) for 39 h in complete medium, washed and treated with NaBt only (5 mM), NaBt plus ActD (10 mg/ml) or ActD alone for 9 h in serum free medium. Cells were collected every hour for 9 h and assayed for the expression of COX-2 by qRT-PCR.

The spontaneous differentiation of Caco-2 cells was carried out as described previously [35]. Briefly, Caco-2 cells were plated and allowed to grow until they reached 100% confluency. These cells were considered as Day 0 cells. Following this, the cells were allowed to grow for 10 or 20 more days with daily changes of the medium to obtain the Day 10 or Day 20 cells. Cells collected at 60% confluency were considered to be proliferating. Cells collected at the respective days were then processed for RNA or protein isolation or transfection.

2.3. RNA isolation and quantitative PCR

RNA isolation was carried out using a NucleoSpin RNA kit (Macherey Nagel, Düren, Germany) according to the manufacturer's instructions. RNA concentration was measured with the BioDrop μLITE (BioDrop, Cambridge, UK). RevertAid First Strand cDNA Synthesis Kit (Thermo Scientific) was used for the synthesis of cDNA synthesis from the RNA. qRT-PCR was carried out in a Bio-Rad CFX Connect (Bio-Rad, Hercules, CA, USA). Reaction conditions for qRT-PCR and product sizes are shown in Supplementary Table 1. To determine the reaction efficiency of the primers used in qRT-PCR, standard amplification curves were generated initially. Expressions of β-Actin or RAB7A were used for normalization.

Prior to qRT-PCR, cDNA was diluted 1:20 with nuclease free dH_2O. The diluted cDNA (2 μl) was mixed with 5 μl 2× Fast Start SYBR Green (Roche, Basel, Switzerland), 0.25 μM forward and reverse primers and made up to a total volume of 10 μl with dH_2O. To determine changes in expression levels, Ct values (threshold cycle) after 40 cycles reaction were calculated by the relative standard curve method. Transcriptional level changes were calculated according to Pfaffl method [36]. MIQE guidelines were followed during the qRT-PCR reactions [37].

2.4. Plasmids and constructs

AU rich RBP binding sequences (Artificial ARE and HuR binding ARE) were cloned at the *BamH1*site into a Super NanoLuc reporter vector. This vector contains the RPSM30 promoter that was reported to be non-responsive to many agents including cytokines [38]. The vector was kindly shared by Prof Khalid S. A. Khabar of the King Faisal Specialist Hospital and Research Centre, Riyadh, Saudi Arabia. The ARE rich region from the 3'UTR of COX-2 was amplified using an MGC Human PTGS2 Sequence-Verified cDNA (Dharmacon, Lafayette, CO, USA) (NCBI Reference Sequence NM_000963.3, 4507 bp mRNA, Catalog no: MHS6278–202756618 Clone ID: 3880850) as a template using Pfu enzyme and cloned into the *BamH1* site of the Super NanoLuc reporter vector. The entire 3'UTR of COX-2 was also amplified from the same cDNA and cloned into the *XhoI* and *NotI* sites of psiCHEK2 vector. For overexpression of HuR, the coding sequence was amplified from the pGEX-6P-1 ELAVL1 expression vector (Dundee University MRC PPU Reagents & Services). A Kozak sequence (5' GCCACC 3′) was introduced immediately upstream of the start codon while a MYC tag (5' GAACA AAAACTCATCTCAGAAGAGGATCTG 3′) was introduced immediately upstream of the stop codon by PCR. The resulting sequence was cloned into the *Sal1* and *Not1* sites of a pGWIZ RPSM30 expression vector. Gene expression in this mammalian expression vector was under the control of the RPSM30 promoter (kindly shared by Prof Khalid S. A. Khabar of the King Faisal Specialist Hospital and Research Centre, Riyadh, Saudi Arabia). All PCR reactions for cloning were carried out using the high fidelity Phusion Taq polymerase (NEB, Ipswich, MA, USA) and all constructs were confirmed by sequencing. Please see Supplementary Table 1 for a list of all oligos and primers used in this study.

2.5. Protein isolation and western blot

M-PER Mammalian Protein Extraction Reagent (Thermo Fisher Scientific) containing 1× protease and phosphatase inhibitors (Roche) was used for the isolation of whole cell extract in accordance with manufacturer's instructions. For the isolation of nuclear and cytoplasmic fractions, the cells were washed twice with ice cold phosphate buffered saline (PBS) and then lysed in 300 μl of a hypotonic buffer containing 10 mM HEPES pH 7.5, 4 mM NaF, 10 μM Na_2MoO_4, 0.1 mM EDTA, 1× protease and phosphatase inhibitors (Roche) and incubated on ice for 15 min. Then, 75 μl of 10% NP-40 (Pan-Reac AppliChem, Darmstadt, Germany) was added, mixed by pipetting up and down and supernatants containing the cytoplasmic fraction were obtained by pulse centrifugation at highest speed for 30 s at 4 °C. The nuclear pellet was resuspended in 80 μl of Nuclear Extraction Buffer containing 10 mM HEPES, pH 7.9, 0.1 mM EDTA, 1 mM DTT, 1.5 mM $MgCl_2$, 420 mM NaCl, 10% glycerol and with 1× protease and phosphatase inhibitors, incubated on ice on an orbital shaker and vortexed for 30 s at 15 min intervals. The lysate was centrifuged for 10 min at 14000 x*g* at 4 °C. The supernatant was considered as the nuclear fraction.

Total (20–50 μg) or cytoplasmic and nuclear proteins (5–10 μg) were separated in 10% SDS-PAGE gels and transferred to PVDF membranes using standard techniques. Bands were visualized with the Clarity ECL Substrate (Bio-Rad) and ChemiDoc MP Imaging System (Bio-Rad). Band intensities were normalized to housekeeping proteins and the results given as "fold change". Topo IIβ or Lamin1B were used as nuclear markers while GAPDH, α-Tubulin or β-actin were used as cytoplasmic or whole cell extract markers. Please see Supplementary Table 2 for a list of all antibodies used in this study.

2.6. Luciferase assay

For luciferase assays to determine 3'UTR activity, Caco-2 and HT-29 cells at 50–60% confluency in 48-well plates were used. The growth medium was changed with Opti-MEM reduced serum medium (Thermo Fisher Scientific). The cells were co-transfected with 40 ng of the NanoLuc reporter vector cloned with ARE sequences and 360 ng firefly reporter vector as an internal control or 40 ng NanoLuc vector cloned with ARE sequences, 80 ng HuR overexpressing vector (or 80 ng empty vector to keep the DNA amounts constant) and 280 ng firefly vector using Lipofectamine 2000 (Invitrogen, Carlsbad, CA, USA) at a 1:2 (plasmid: transfection reagent) ratio according to manufacturer's instructions. After 6 h (for Caco-2 cells) or 24 h (for HT-29 cells) incubation at 37 °C, the transfection medium was removed and replaced with complete medium containing 5 mM NaBt or vehicle (control) for 48 h. For the analysis of Firefly and NanoLuc activities Nano-Glo Dual Luciferase Reporter Assay System (Promega, Madison, WI, USA) was used according to the manufacturer's instructions and the activities were measured by a luminometer (Turner Biosystems, Thermo Fisher Scientific).

2.7. RNA immunoprecipitation (RNA IP)

RNA IP was carried out according to the protocol of Peritz et al. 2006 [39]. To evaluate the binding of endogenous HuR protein to an HuR binding ARE sequence, HCT-116 in T25 flasks were transfected with 3.5 μg of a NanoLuc vector in which the HuR binding sequence was cloned. 10 μl Lipofectamine 2000 (Invitrogen) was used and the transfection was carried out for 6 h after which the cells were either treated with either 5 mM NaBt or vehicle (water) for 48 h in complete medium. To determine the binding of endogenous HuR to the 3'UTR of

COX-2, Caco-2 cells in T25 flasks were treated with 5 mM NaBt or vehicle for 48 h. For each RNA immunoprecipitation, 5×10^6 cells were used; for input, 3×10^5 cells were used. Cells were lysed with 1 ml polysome lysis buffer (PLB) [100 mM KCl, 5 mM $MgCl_2$, 10mMm HEPES, pH 7.0, 0.5% Nonidet P-40, 1 mM DTT, 100 Uml^{-1} RNasin RNase inhibitor (Promega), 2 mM vanadyl ribonucleoside complexes solution (Sigma), 25 µl ml^{-1} protease inhibitor cocktail (Roche)]. Next, 50% Protein A/G magnetic beads (Thermo Scientific) were equilibrated by washing the beads with 500 µl of PLB twice and then restoring the original volume with the same buffer (PLB). The bead slurry was separated into three aliquots of 50 µl each. Two of the aliquots were used for pre-clearing while the other aliquot was used for incubation with the antibody bound cell lysate. First, one aliquot of the pre-clearing slurry was added to 1 ml of cell lysate and incubated with rotation at 4 °C for 1 h. After incubation, the beads were collected with a magnetic rack. The collected supernatant was incubated with the second pre-clearing aliquot of bead slurry with rotation at 4 °C for 1 h. Next, the supernatant was incubated with 4 µg of α-HuR (ProteinTech, Manchester, UK, Cat no: 66549–1-Ig) or 4 µg of mouse IgG (Santa Cruz, Cat. no: sc-2025) with rotation at 4 °C overnight. The next day, the third aliquot of the bead slurry was added to this cell lysate and incubated with rotation at 4 °C for 4 h. The beads were collected using the magnetic rack and the supernatant was removed. The beads were washed with 500 µl PLB four times with rotation at 4 °C for 5 min for each wash, followed by 4 more washes with PLB containing 1 M urea with rotation at 4 °C for 5 min each. The beads were next re-suspended with 100 µl PLB containing 0.1%SDS and 30 µg proteinase K and incubated at 50 °C for 30 min. One volume (100 µl) of phenol-chloroform-isoamyl alcohol mixture was added and vortexed. To separate the phases, the beads were centrifuged. The upper phase was taken to a fresh eppendorf tube and 5 µl glycogen (20 mg/ml), 12 µl 3 M sodium acetate and 250 µl 100% ethanol were added to 100 µl of the upper phase and mixed. The mixture was incubated at −20 °C overnight for ethanol precipitation. The mixture was centrifuged for 20 min at 4 °C at 16000 ×*g*. Ethanol was removed and the pellet was allowed to air-dry, re-suspended in RNase free water and stored at −80 °C.

The immunoprecipitated RNA samples were converted to cDNA and analyzed by qRT-PCR using primers spanning the Super NanoLuc luciferase sequence of the vector or the coding sequence as well as 3'UTR region of COX-2 (please see Supplementary Table 1 for primer sequences and product sizes). The primer sequences to determine the binding of HuR to the 3'UTR of eIF4E (positive control) was obtained from Topisirovic et al. [40]. First, a standard amplification curve was generated using the input cDNA and accordingly the dilution factor was determined as 1:500. The input Ct value was determined by extracting the transformation of dilution factor in logarithmic scale base 2 from the measured input Ct value of both treated and untreated samples. The ΔCt value was calculated by extracting the calculated input Ct value from the Ct values of immunoprecipitated samples. For untreated samples, untreated input Ct value was used and for treated samples, treated input Ct value was extracted. Mean of ΔCt values of IgG precipitated samples was calculated and ΔΔCt value was calculated for treated and untreated samples separately by extracting the mean value from ΔCt of IgG and HuR precipitated samples. The fold change of HuR precipitated samples compared to IgG precipitated samples was calculated for both untreated and NaBt treated samples.

2.8. Statistical analyses

All experiments were repeated at least 2–3 times independently, with 3–6 technical replicates in each independent replicate and represented as mean ± standard error of mean (SEM). Unless otherwise indicated, statistical analyses between experimental results were based on ANOVA or unpaired *t*-test. Statistical analyses and graphing were carried out using GraphPad Prism (La Jolla, CA, USA). A p value ≤ 0.05 was considered as statistically significant.

3. Results

3.1. In silico analyses showing global repression in the expression of RBPs in cells treated with sodium butyrate

Publicly available microarray datasets obtained from work with HT-29 (GSE45220) or HeLa (GSE17397) cells treated for 24 h with 2 mM NaBt (HT-29) or for 15 h with 5 mM NaBt (HeLa), were analyzed for the expression of RBPs. For GSE45220, a total of 446 probes representing 395 unique human RBPs (hRBPs) were extracted from the expression matrix. Differential expression analysis (FDR < 0.1) showed that NaBt treatment resulted in an overall greater downregulation of RBPs (80 genes) compared to their upregulation (13 genes) (Fig. 1A, list of all genes are given in Supplementary Table 3). For GSE17397, a total of 388 unique probes representing 366 unique hRBPs were extracted from the expression matrix. Similar to the HT-29 data, differential expression analysis (FDR < 0.1) showed that NaBt treatment resulted in an overall greater downregulation of RBPs (80 genes) compared to their upregulation (22 genes) (Supplementary Fig. 1A, list of all genes are given in Supplementary Table 3).

To determine whether the expression of RBPs in cells treated with NaBt was temporally regulated, the publicly available microarray data (GSE4410) obtained from work with a immortalized non-transformed mouse colon epithelial cell line treated for 0, 6, 12 and 24 h with 2 mM sodium butyrate (NaBt) was analyzed for the expression of RBPs [24]. Differential expression analysis ($p < 0.05$) indicated that NaBt treatment again resulted in an overall greater downregulation of RBPs (117 genes) compared to their upregulation (43 genes) (List of all genes are given in Supplementary Table 3). Of these, 25 genes were significantly downregulated at every time point while 9 genes were significantly upregulated at every time point (Supplementary Fig. 1B). Volcano plots of RBP genes significantly up and down-regulated in the presence of NaBt indicated that the effect was highly temporal with a stronger downregulation observed at longer time points (Supplementary Fig. 1C, list of all genes are given in Supplementary Table 3).

We next queried whether the genes that were significantly down and upregulated in the presence of NaBt formed a signaling network. Data from GSE45220 indicated while the RBPs that were downregulated in HT-29 cells treated with 2 mM NaBt formed a tight network indicating that these genes were part of a closer and more extensive interaction network, the RBPs that were upregulated did not form a significant interaction network (Fig. 1B). MCE301 cells (GSE4410) also showed the same trend with the downregulated RBP genes showing a stronger interaction network compared to the upregulated genes, which increased as the duration of treatment was increased (Supplementary Fig. 1D).

3.2. Downregulation of several RBPs in NaBt treated colon cancer cell lines

To confirm the in silico data that indicated downregulation of many RBPs, we treated colon cancer cell lines Caco-2 and HT-29 with 3 and 5 mM NaBt for 48 h followed by the isolation of whole cell lysates as well as nuclear and cytoplasmic fractions. An MTT assay indicated that Caco-2 cells retained around 77 ± 4% and 64 ± 2% of cell viability when treated for 48 h with 3 mM and 5 mM NaBt, respectively. HT-29 cells retained 40 ± 3% and 32 ± 6% of viability when treated for 48 h with 3 mM and 5 mM NaBt, respectively (Supplementary Fig. 2). We next examined the expression of four RBPs, AUF1, CUGBP2, TIAR and HuR that are known to bind to the 3'UTR of COX-2 [11]. These genes showed reduced expression (AUF1, CUGBP2 and TIAR), or no change in expression (HuR) in the HT-29 dataset (GSE45220, Supplementary Fig. 3). Confirming the in silico data, the cytoplasmic, nuclear and whole cell extract (WCE) levels of the destabilizing proteins AUF1 (Fig. 2A), CUGBP2 (Fig. 2B) and TIAR (Fig. 2C) were observed to decrease in NaBt treated HT-29 and Caco-2 cells. Interestingly, treatment of HT-29 cells with 3 and 5 mM NaBt treatment did not lead to any

decrease in expression of the stabilizing protein HuR; rather, a reduction in the cytoplasmic levels of the protein was observed (Fig. 2D), corroborating the lack of any change of mRNA expression seen in GSE45220 (Supplementary Fig. 3). In Caco-2 cells there was a reduction in nuclear as well as whole cell extract of the protein; however, no significant alteration was observed in the cytoplasmic levels (Fig. 2D).

To confirm the role of NaBt in modulating 3'UTR activity using a reporter assay, we chose two different RBP binding sequences: 1) An artificial ARE sequence [41], which could bind to several different RBPs such as HuR, HuB and TTP as indicated by an analysis of the sequence using the database for RNA binding protein specificities RBPDP (http://rbpdb.ccbr.utoronto.ca/) 2) An artificial ARE sequence consisting of binding sequences for the RBP HuR only. Each of these sequences were cloned into an RPSM30 NanoLuc reporter vector [38]. This vector was designed with a ribosomal protein (RPSM30) promoter that was shown to respond minimally at the transcriptional level to many different treatments [38]. In the current study, using cells transfected with the empty vector and treated with 5 mM NaBt, we observed that this promoter was non- responsive to NaBt; whereas the SV40 promoter in the psiCHEK2 vector was strongly responsive to NaBt (Supplementary Fig. 4A). When we transfected Caco-2 cells with each of these constructs there was a dramatic increase in luciferase activity in both ARE sequences (Fig. 3A). This indicated that stabilizing proteins such as HuR, were functional in these cells. Importantly, when we treated the cells with 5 mM NaBt for 48 h, we observed a very significant decrease in the luciferase activity, confirming that there was an overall suppression in the activity of endogenous stabilizing RBPs in Caco-2 cells in the presence of NaBt (Fig. 3A).

To further confirm whether the treatment with NaBt was able to suppress stabilizing RBPs, we transfected Caco-2 and HT-29 cells with an HuR overexpressing construct along with the HuR binding ARE sequence (Fig. 3B). For both cell lines we observed that when HuR was overexpressed, a significant increase in luciferase activity was observed as expected, confirming the RNA stabilizing effect of HuR. When the cells were treated with NaBt, a strong suppression of reporter activity was seen indicating that even when HuR was found in abundance, NaBt

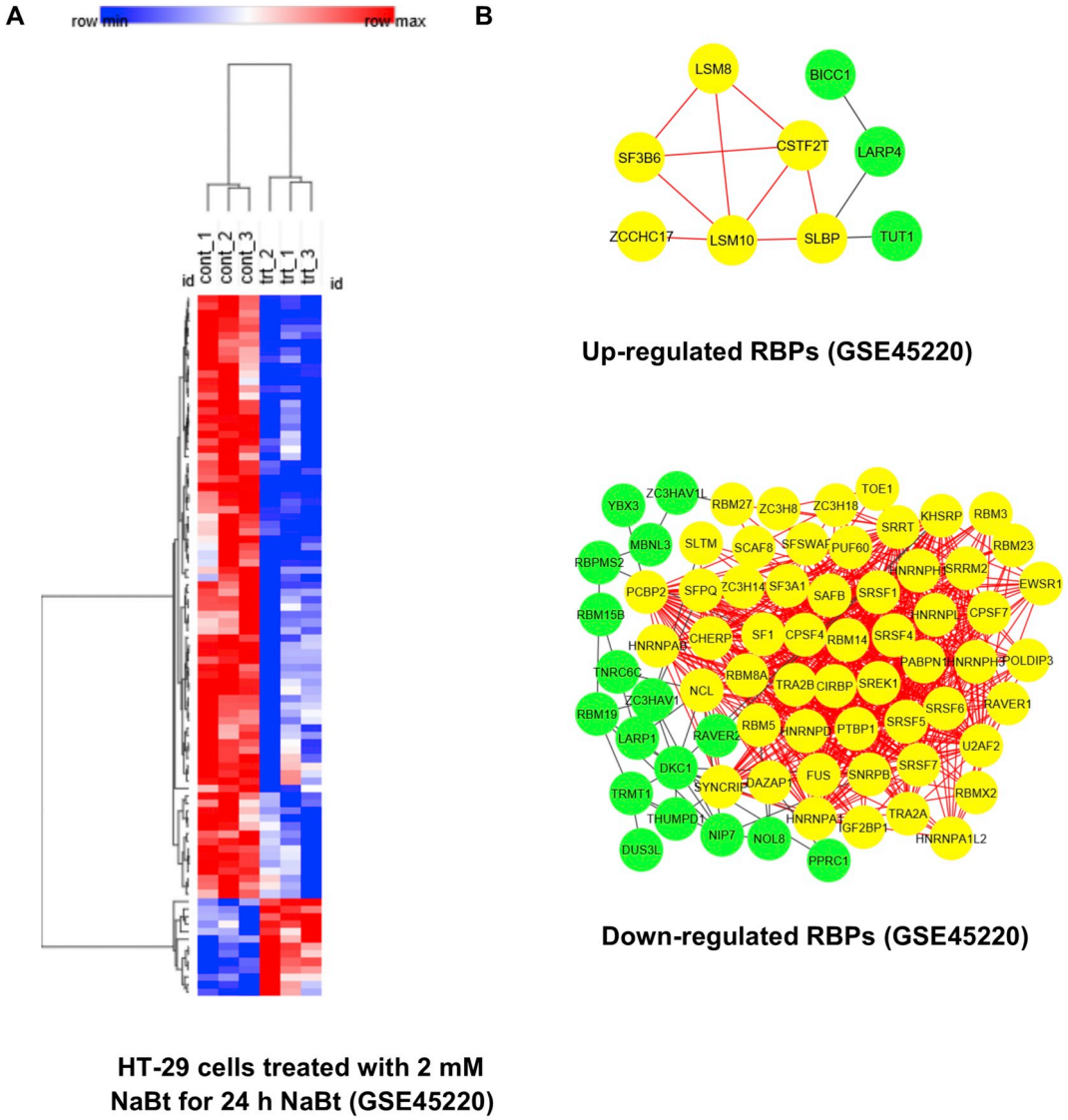

Fig. 1. Analysis of microarray data of HT-29 cell line (GSE45220) showing differential expression of RBPs in the presence of NaBt. (A) Heatmap of significantly differentially expressed RBPs showing downregulated (80) and upregulated (13) genes upon NaBt treatment. Heatmap was generated by Morpheus software, Broad Institute (https://software.broadinstitute.org/morpheus/). (B) STRING network analysis showing that the downregulated RBPs (upper panel) after 24 h of treatment with NaBt form a complex and highly interconnected interaction network as compared to the upregulated RBPs (lower panel). Yellow color represents the genes forming the core of the interaction network based on clustering analysis on Cytoscape. (For interpretation of the references to color in this figure legend, the reader is referred to the web version of this article.)

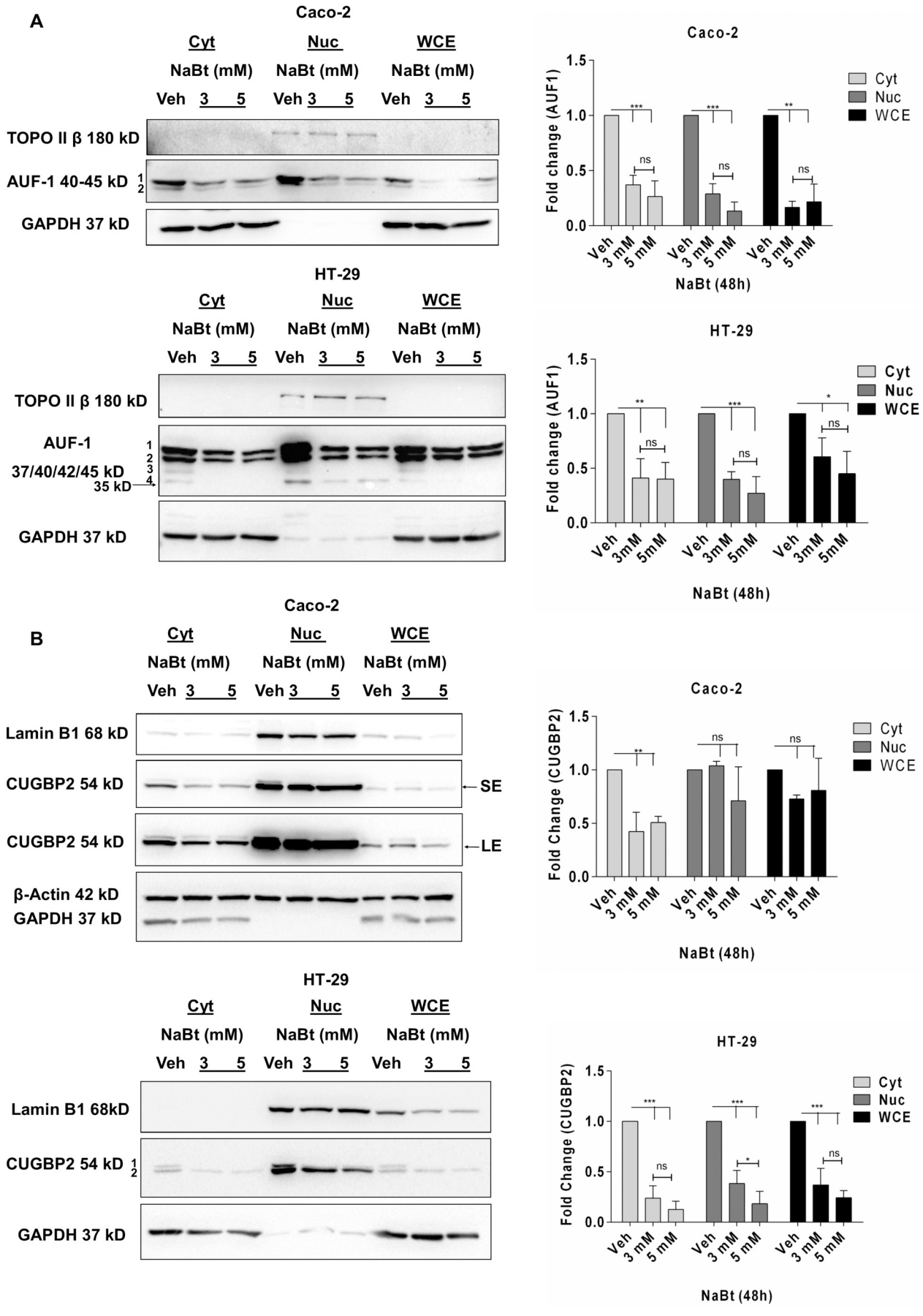

(caption on next page)

Fig. 2. Expression of RBPs in HT-29 and Caco-2 cells treated with NaBt. Caco-2 (upper panels) and HT-29 (lower panels) cells were treated for 48 h with NaBt followed by the isolation of nuclear and cytoplasmic fractions as well as whole cell extract (WCE). (A) The expression of two different AUF1 isoforms in Caco-2 and four different isoforms in HT-29 are shown. Expression of (B) CUGBP2 (C) TIAR and (D) HuR are shown. The experiments were repeated at least three times independently and densitometric analyses showing fold change in expression in the NaBt treated cells with respect to the vehicle treated cells are shown. Statistical analyses were carried out using ANOVA followed by Tukey's multiple comparisons test. TOPOIIβ or Lamin B1 were used as nuclear loading controls while GAPDH was used as the cytoplasmic loading control. $*P < 0.05$, $**P < 0.01$, $***P < 0.001$, ns: not significant.

could suppress the stabilizing function.

Next, we carried out an RNA immunoprecipitation (RNA IP) to determine whether the binding of HuR to a target ARE sequence was affected in the presence of NaBt. For this we transfected HCT-116 cells with the HuR binding ARE construct for 6 h, followed by treatment with 5 mM NaBt or vehicle for 48 h and then carried out the RNA IP assay. HCT-116 cells were selected for this assay as these cells are very easy to transfect and, similar to HT-29 cells, showed a decrease in cytoplasmic levels of HuR when treated with NaBt (Supplementary Fig. 4B). We observed a significant decrease in the binding of endogenous HuR to its binding sequence in the presence of NaBt compared to the vehicle treated cells (Fig. 3C). The binding of HuR to the 3'UTR of eIF4E was used as a positive control [40].

3.3. Signaling cascade for HuR translocation in the presence of NaBt

The translocation of HuR from the nucleus to the cytoplasm is a closely regulated event [16] . Since we observed a decrease in both cytoplasmic translocation of HuR and its binding to target sequences in the presence of NaBt, we hypothesized that treatment with NaBt may affect signal transduction pathways that regulate the nucleo-cytoplasmic shuttling and 3'UTR binding of HuR. It is known that both cytoplasmic translocation and binding to target mRNA sequences is regulated by the activation through phosphorylation of a p38 MAP Kinase-MAPKAPK2 (MK2) signaling axis for the stabilization of a number of inflammatory mRNAs such as COX-2 and TNFα [42,43]. We observed that in both Caco-2 and HT-29 cells, treatment with 1, 3 and 5 mM NaBt for 48 h resulted in a decrease in phosphorylation of p38 (Fig. 4A) while the levels of the total proteins remained the same. Both total and phosphorylated levels of MK2 decreased in the Caco-2 cells, whereas for HT-29 cells there was a decrease in the levels of phosphorylated MK2, and to a lesser extent the total MK2. This indicates that the decrease in activation of the p38-MK2 signaling axis could be associated with the reduction in the cytoplasmic translocation of HuR as seen in HT-29 cells or reduced binding to HuR target mRNA sequences as seen in Caco-2 cells. Interestingly, very slight fluctuations (Caco-2) or no change (HT-29) in the phosphorylation of MK2 was observed in cells treated with another HDAC inhibitor suberoylanilide hydroxamic acid (SAHA) (Supplementary Fig. 5A) indicating that the effect of NaBt in this signaling network may not be related to the inhibition of HDAC activity.

It has been shown previously that the translocation of HuR can also be regulated through phosphorylation by the stress related kinase Chk2 in a cell cycle dependent manner [15,16]. Since the cytoplasmic translocation of HuR was reduced in HT-29 cells, we first examined whether NaBt treatment resulted in cell cycle arrest in these cells. HT-29 cells that were overnight starved for synchronization showed an increase in the proportion of G1 cells indicating a G1/S arrest as expected; the same cells after release into complete medium for 12 h showed a decrease in G1 phase cells indicating that the cells were cycling again and that the starvation model was suitable for synchronization (Supplementary Fig. 5B). We observed that many more of the synchronized cells treated with 5 mM NaBt for 3, 6, 9 and 12 h were in the S and G2/M phases compared to the control (vehicle) treated cells that were in G1 phase (Supplementary Fig. 5C). The cell cycle check point protein Chk2 is known to induce cell cycle arrest at S and G2/M in the presence of DNA damaging agents [44] and was shown to phosphorylate HuR at S88, S100, and T118; moreover, these phosphorylations were shown to dissociate HuR from the 3'UTR of a target mRNA [45]. We have observed that concomitant with increased number of cells at S and G2/M, synchronized HT-29 cells treated with NaBt also underwent enhanced phosphorylation of Chk2 after 3-12 h of treatment (Fig. 4B). Longer time points (beyond 12 h) were not examined for the phosphorylation of Chk2 as the cells were most likely to not be synchronized any more. At the 6 h time point, when we observed the highest phosphorylation of Chk2 in HT-29 cells, we also observed a very strong decrease in the cytoplasmic levels of HuR (Fig. 4C). Interestingly, synchronized Caco-2 did not show any change in the phosphorylation of Chk2 after 6 h of treatment with NaBt (Fig. 4D), supporting idea that p38/MK2 mediated reduction in mRNA binding was likely to be more functional in regulating HuR activity in these cells. It is also possible that the progression of the cell through different stages of the cell cycle in Caco-2 cells is different from HT-29 and alterations in the phosphorylation of Chk2 occur at different time intervals.

3.4. NaBt treatment can post transcriptionally regulate the expression of inflammatory mRNAs

To determine the functional consequences of NaBt mediated regulation of RBP expression and activity, we chose COX-2 as a candidate mRNA that is known to be regulated post transcriptionally by RBPs [10]. We treated Caco-2 and HT-29 cells that are known to express COX-2 [46] with different doses (1-5 mM) of NaBt for 6- 48 h and observed a significant decrease in the expression of COX-2 in the presence of NaBt in both Caco-2 (Fig. 5A for 48 h of treatment, Supplementary Fig. 6A for other time points) and HT-29 (Fig. 5B for 48 h of treatment, Supplementary Fig. 6B for other time points) cells. These data indicate that the expression of COX-2 was decreased as early as 6 h and remained suppressed at 48 h of treatment. The expression of COX-1, which has housekeeping functions and is regulated differently from COX-2, was seen to increase with NaBt treatment in both HT-29 and Caco-2 cells (Supplementary Fig. 6C). Since the expression of COX-2 can be regulated at both transcriptional [47] and post-transcriptional [18] levels by NaBt, we first determined the activity of the transcription factor NF-κB that is known to transcriptionally upregulate COX-2 genes during an inflammatory response [26]. Treatment of Caco-2 cells for 6 h with NaBt did not lead to any alteration in NF-κB transcriptional activity as observed with a luciferase assay but treatment with NaBt for 48 h showed an increase in transcriptional activity (Fig. 5C, left panel). HT-29 cells, treated for the same duration (48 h) and dose (5 mM) of NaBt showed a decrease in transcriptional activity (Fig. 5C, right panel). We also examined the nuclear translocation of the p65 subunit of NF-κB and observed that 48 h NaBt treated Caco-2 cells had greater nuclear levels of p65 whereas the 48 h NaBt treated HT-29 cells showed no difference in nuclear p65 levels compared to vehicle treated cells (Fig. 5D). These data indicate that the transcriptional activity of NF-κB could not be accounted directly for the decrease in expression of COX-2 observed in the presence of NaBt suggesting the involvement of, among other mechanisms, post transcriptional regulation. We therefore carried out an Actinomycin D (ActD) chase assay with HT-29 cells. This cell line was selected for the assay as we observed an inhibition of NF-κB activation as well as alterations in both signaling pathways i.e. the reduction in phosphorylation of p38-MK2 and the increase in phosphorylation of Chk2 in these cells. In the NaBt + ActD treated cells, we observed a decrease in the COX-2 mRNA levels at the early time points of treatment with ActD indicating the loss of new mRNA synthesis [48]. In

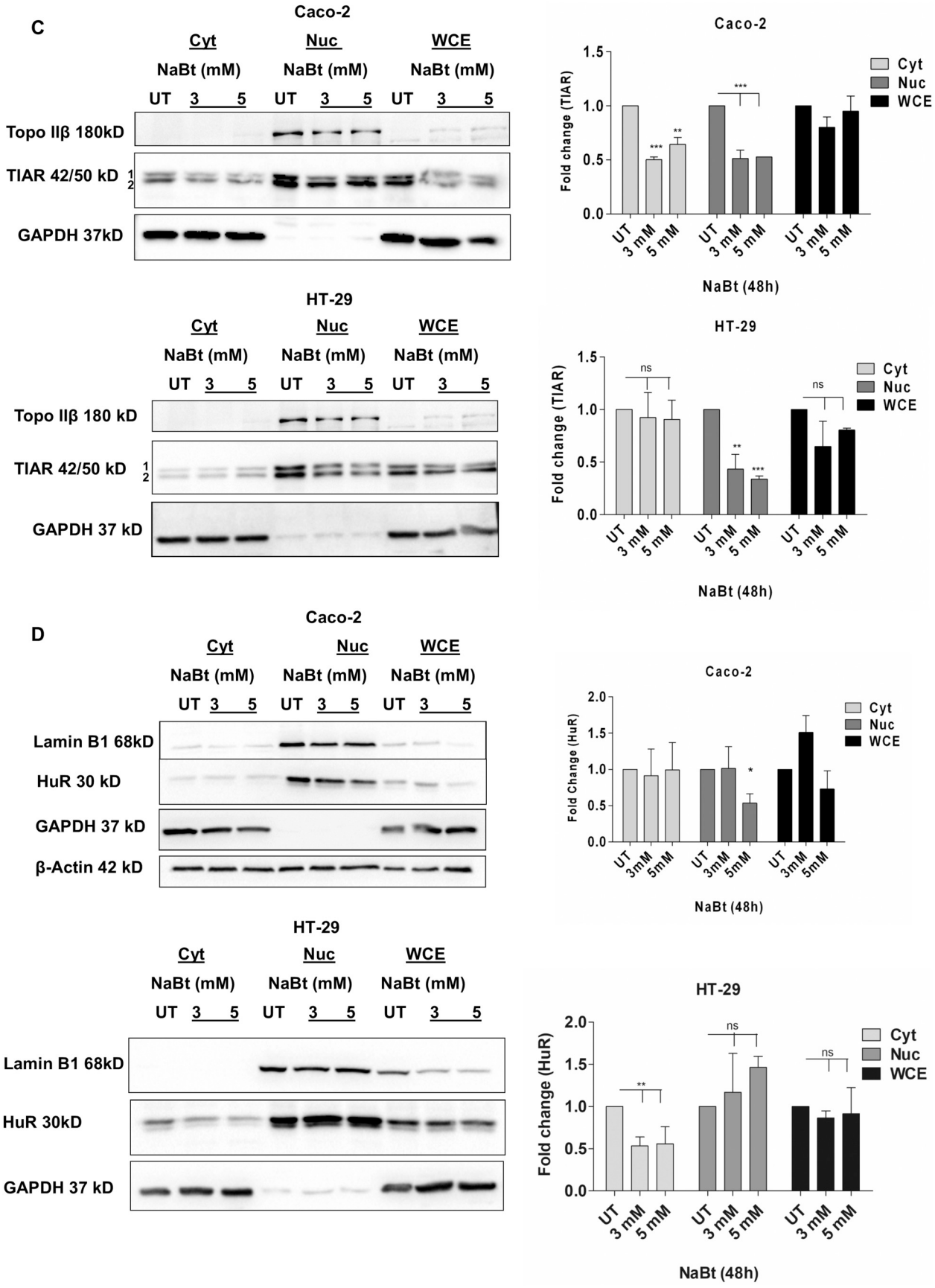

Fig. 2. (*continued*)

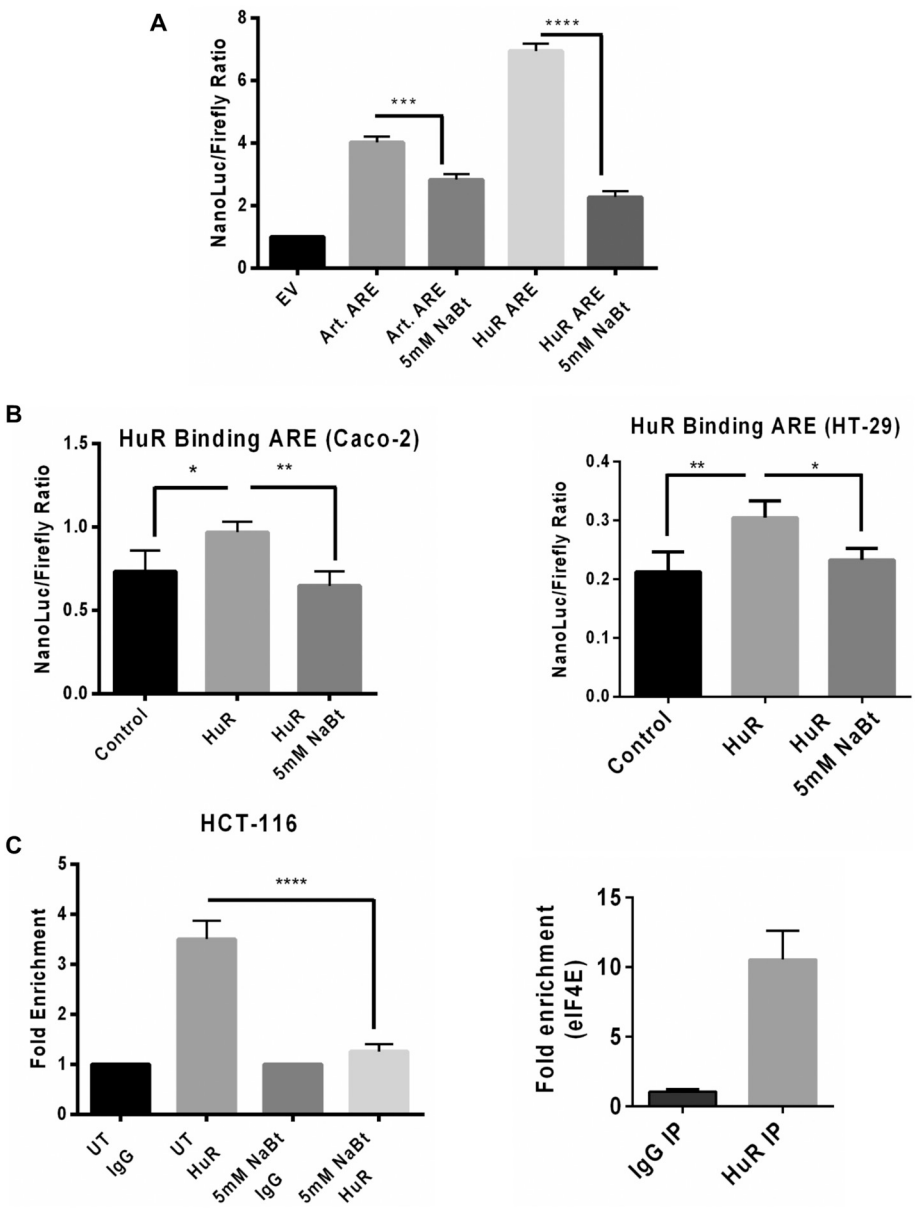

Fig. 3. Effect of NaBt on 3'UTR activity of different ARE sequences. Caco-2 or HT-29 cells were treated with 5 mM NaBt for 48 h and transfected with these constructs separately or the empty vector for 24 h. The cells were then collected and processed for luciferase activity. A vector encoding the firefly luciferase gene was used as a normalization control. (A) Caco-2 cells transfected with an artificial ARE sequence that binds to several RBPs and an artificial ARE sequence that solely binds to HuR showed suppression in 3'UTR activity in the presence of NaBt. (B) Caco-2 or HT-29 cells transfected with the HuR ARE showed stabilization of the reporter when the cells were transfected with an HuR overexpression vector. This stabilization was lost when the cells were also treated with 5 mM NaBt. (C) RNA IP showing reduced enrichment of HuR binding ARE sequences in 5 mM NaBt treated cells HCT-116 compared to vehicle treated cells. Right panel: Positive control for RNA IP for enrichment of HuR binding to the 3'UTR of eIF4E. Statistical analyses of two independent biological replicates was carried out by ANOVA followed by Tukey's multiple comparison test.

the following hours, however, the NaBt + ActD treated cells showed a significantly greater decrease in the COX-2 mRNA levels compared to the ActD alone or NaBt alone treated cells, indicating destabilization of the mRNA (Fig. 5E). To determine the half-life of the COX-2 mRNA from the ActD chase assay, trend lines were generated according to best fit for the graph of time (in minutes) versus expression. For the expression data from ActD treated cells, a polynomial equation was obtained ($y = 1197.2 \times {}^{2}$–$1974.8\times + 776.56$, $R^2 = 0.972$). For the expression data from NaBt treated cells, a linear equation was obtained ($y = -421.52\times + 412.35$, $R^2 = 0.2631$). For the expression data from NaBt + ActD treated cells, a logarithmic equation was obtained ($y = -149\ln(x) - 77.639$, $R^2 = 0.7329$). According to these equations, the half-life of the COX-2 mRNA was determined as 88 min for ActD treated cells, 202 min for NaBt treated cells and 30 min for NaBT + ActD treated cells.

Next, we examined the activity of the ARE binding sequences from the 3'UTR of COX-2 using the NanoLuc reporter assay. Here we used Caco-2 cells since these cells are easier to transfect compared to HT-29 cells and showed reduced reporter activity in the presence of NaBt when transfected with an artificial ARE sequence (Fig. 3A). When Caco-2 cells were transfected with the COX-2 ARE sequence along with the HuR overexpression vector, significant increase in the luciferase activity was observed, indicating stabilization of the mRNA. More importantly, treatment of the cells with 5 mM NaBt for 48 h resulted in a significant decrease in the luciferase signal suggesting the inhibition of HuR activity and therefore destabilization (Fig. 5F). We also carried out an RNA IP to determine effect of NaBt on the endogenous binding of HuR to the 3'UTR of COX-2. While we could successfully precipitate HuR-bound 3'UTR sequences of COX-2 in the vehicle treated cells, the precipitation was dramatically reduced in the cells treated with 5 mM NaBt (Fig. 5G). Minimal precipitation was observed with isotype specific IgG. Finally, overexpression of HuR resulted in an increase in the protein levels of COX-2, most likely due to stabilization of the COX-2 mRNA. When the HuR overexpressing cells that were treated with butyrate, the COX-2 protein levels were reduced further suggesting an inhibition of HuR activity in the presence of butyrate (Fig. 5H).

NaBt treatment has been reported to induce differentiation in Caco-2 cells [49]. To determine whether treatment with NaBt for 48 h could induce differentiation in Caco-2 cells and whether this differentiation had any effect on the post transcriptional regulation of COX-2, we first determined the expression of differentiation markers. Treatment of Caco-2 cells with 3 and 5 mM NaBt resulted in a 1.5–2-fold increase in

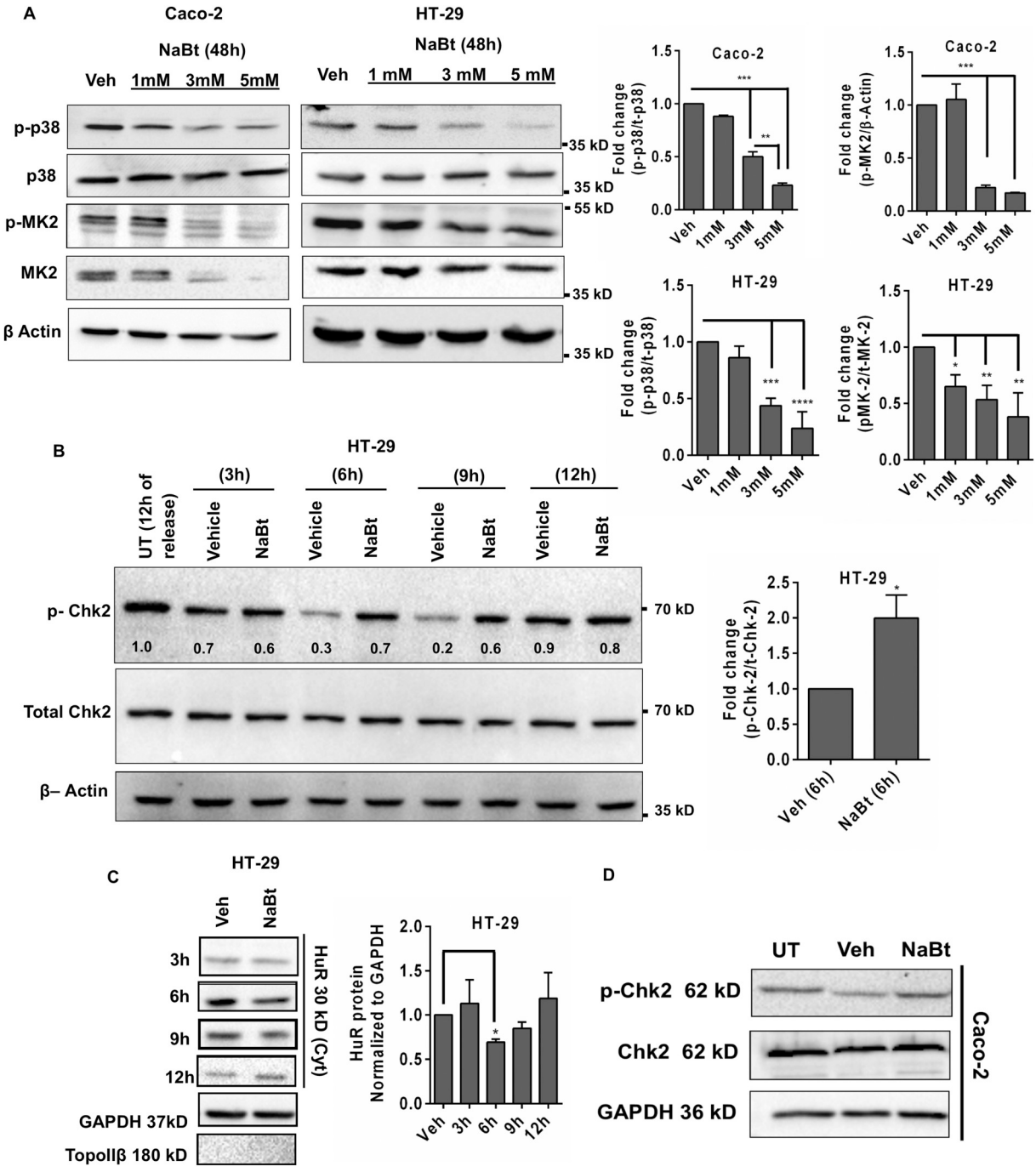

Fig. 4. Signal transduction pathway for the reduced cytoplasmic translocation of HuR in the presence of NaBt (A) Reduced phosphorylation of p38 and MK-2 in Caco-2 (left panel) and HT-29 (right panel) cells treated with NaBt for 48 h. (B) Increased phosphorylation of Chk2 in HT-29 cells treated with NaBt for 3, 6, 9 and 12 h. HT-29 cells were starved overnight and then released in 10% serum containing medium for 12 h (UT). The cells were then treated with either vehicle or NaBt for 3-12 h. The proteins were collected and assayed for phosphorylation of Chk2. Statistical significance was determined with *t*-test (*$p < 0.05$). (C) Cytoplasmic levels of HuR in synchronized HT-29 cells treated with NaBt for 3-12 h. HT-29 cells were serum starved overnight and then released in 10% serum containing medium for 12 h. The cells were then treated with either vehicle or NaBt for 3-12 h. Cytoplasmic proteins were collected and assayed for HuR by Western blot. (D) Lack of change in phosphorylation of Chk2 in synchronized and released Caco-2 cells treated with NaBt for 6 h. Densitometric analysis was carried out with respect to the vehicle treated cells and normalized to the loading control (β-actin). Statistical analyses of three independent biological replicates was carried out by ANOVA followed by Tukey's multiple comparison test.

the expression of sucrose isomaltase (SI) (Supplementary Fig. 7A). Caco-2 cells were also spontaneously differentiated by growing 100% confluent cells (Day 0) for 10 (Day 10) or 20 (Day 20) more days so that the cells can undergo differentiation [35]. Post-confluent differentiated Caco-2 cells led to an increase in SI expression of over 400 fold (Supplementary Fig. 7A). We also determined the protein expression of carcinoembryonic antigen (CEA) and again observed a modest increase in expression in 3 and 5 mM NaBt treated cells compared to a more dramatic increase in spontaneously differentiated cells (Supplementary Fig. 7B). These data indicate that NaBt treatment did induce differentiation-like features in Caco-2 cells, but the change in expression of the markers was more modest compared to the spontaneously

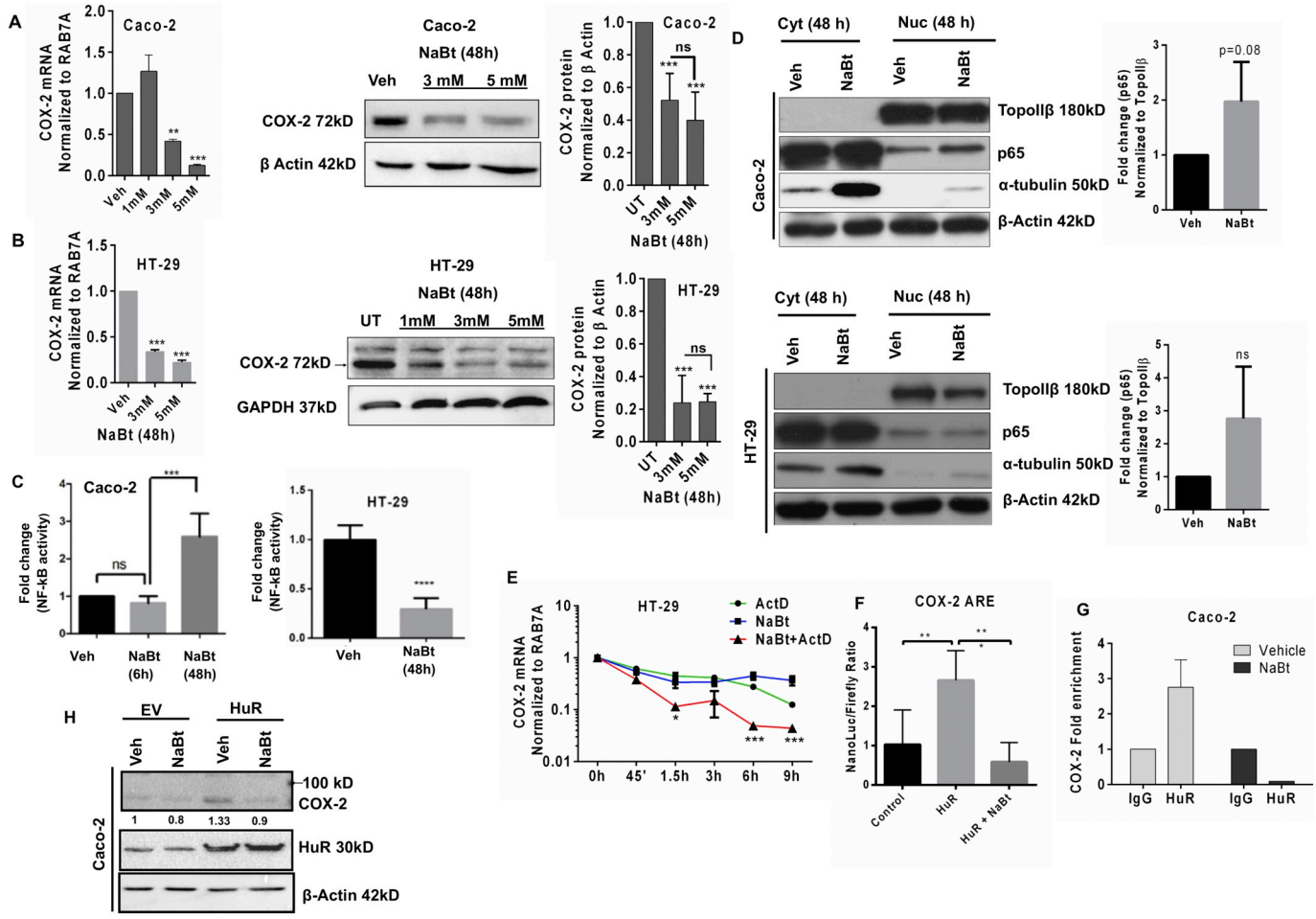

Fig. 5. COX-2 expression can be downregulated post-transcriptionally via reduced HuR binding in NaBt treated cells. mRNA and protein expression of COX-2 in (A) Caco-2 and (B) HT-29 cells treated with different concentrations of NaBt for 48 h. (C) Luciferase assay showing no change in NF-κB transcriptional activity after 6 h treatment with NaBt and an increase in activity after 48 h treatment with NaBt in Caco-2 cells. 48 h NaBt treatment led to a significant decrease in NF-κB activity in HT-29 cells (t-test, $***P > 0.001$, $****P < 0.0001$). (D) Western blot indicating that nuclear level of NF-κB p65 was increased in 5 mM NaBt treated Caco-2 cells; no alteration was seen in HT-29 cells. (E) ActD chase assay showing greater reduction in COX-2 mRNA levels of cells treated with ActD (10 mg/ml) + NaBt (5 mM) compared to NaBt or ActD alone. (ANOVA with Tukey's post hoc test, $*P < 0.05$, $***P < 0.001$) (F) Luciferase reporter assay showing stabilization of ARE sequences in the 3'UTR of COX-2 with HuR overexpression in Caco-2 cells; treatment with 5 mM NaBt resulted in a significant reduction in luciferase activity even with HuR overexpression. (G) RNA IP showing reduced enrichment of HuR binding sequences from the COX-2 3'UTR when Caco-2 cells were treated with 5 mM NaBt. (H) Western blot showing increased protein expression of COX-2 in HuR overexpressing Caco-2 cells. This increase in expression was reversed when the cells were treated with 5 mM NaBt.

differentiated cells. We next determined COX-2 expression in the spontaneously differentiated cells and observed a significant decrease in expression of COX-2 at both mRNA and protein levels in the spontaneously differentiated cells compared to the proliferating and Day 0 confluent cells (Supplementary Fig. 7C). To determine whether the decrease in expression of COX-2 was regulated via the 3'UTR, we transfected proliferating, confluent (Day 0) and differentiated (Day 10) cells with a reporter vector (psiCHEK2) in which the entire 3'UTR of COX-2 was cloned. We used the psiCHEK2 vector instead of the NanoLuc vector with the RPSM30 promoter for two reasons: first, as the spontaneous differentiation of Caco-2 cells did not require treatment with any agents, we could disregard the possibility of aberrant promoter activation. Secondly, differentiated Caco-2 cells are relatively more challenging to transfect. Therefore, by using the psiCHEK2 vector, which has both Renilla and Firefly sequences, we only needed to transfect the cells with a single plasmid. We observed that the 3'UTR activity of COX-2 remained identical independent of whether the cells were proliferating, confluent or differentiated (Supplementary Fig. 7D), indicating that the regulation during differentiation was primarily transcriptional. This also corroborates with our previous findings [50] of reduced transcriptional activation of NF-κB in the differentiated Caco-2 cells compared to the undifferentiated cells. It is thus likely that reduced activity of transcription factors could have resulted in the reduced expression of COX-2 in the spontaneously differentiating model.

4. Discussion

Butyric acid is a short chain fatty acid (SCFA), which, along with propionic acid and acetic acid, is generated in copious amounts by the gut microbiome using dietary fibers [6], estimated to be between 70 and 140 mM in the proximal colon and 20-70 mM in the distal colon [51] depending on the diet. Considering a ratio of acetate:propionate:butyrate 60:20:20 [52], the level of butyrate is expected to be between 14 and 28 mM in the proximal colon and 4–14 mM in the distal colon. Many of the beneficial functions of butyrate have been attributed to its ability to inhibit histone deacetylases (HDACi) [53]; moreover, a few studies have indicated that the HDACi function of butyrate may regulate the expression of RNA binding proteins, thereby modulating mRNA stability and gene expression [18,54]. We therefore aimed to examine whether regulation of gene expression in the

presence of butyrate may be carried out through post-transcriptional alterations in mRNA stability. We first carried out an in silico analysis of publicly available microarray datasets (GSE45220 [23], GSE4410 [24] and GSE17397 [25]) for the expression of different RBPs in epithelial cells treated with NaBt and observed that the expression of most RBPs (but not all) was reduced in the NaBt treated cells compared to control. Confirmatory experiments indicated that the expression as well as cytoplasmic translocation of several RBPs, irrespective of their destabilizing or stabilizing function, were reduced in Caco-2 and HT-29 cells treated with NaBt. Using reporter assays, we further confirmed that the expression of a luciferase gene could be suppressed in the presence of butyrate via ARE sequences cloned downstream of the reporter gene.

To better understand the mechanism of suppression of the reporter gene expression, we focused on the RNA binding protein HuR. HuR was selected as the candidate RBP in the current study since it is already known to stabilize mRNAs related to diverse cellular and biological process including inflammation. Additionally, the microarray dataset GSE45220 [23] and our wet lab data indicated that the expression of HuR was not altered in the presence of butyrate; rather, its cytoplasmic translocation was affected. Interestingly, although Caco-2 and HT-29 cells treated with SAHA showed a reduction in COX-2 mRNA and protein levels (data not shown), we did not observe any activation of the p38-MK2 pathway in these cells treated with SAHA. This suggest that post-transcriptional regulation of gene expression may not solely be mediated via changes in gene expression of RBPs via the HDAC inhibitory activity of butyrate. The phosphorylation of p38 and its downstream activator MK2 were reduced in both Caco-2 and HT-29 cells treated with butyrate. Phosphorylation of HuR at T118 by p38/MK2 was shown to enhance the cytoplasmic translocation of HuR [55] leading to the stabilization of inflammatory mRNAs [56]. Of note, in spite of a lack of alteration in the cytosolic levels of HuR in Caco-2 cells treated with butyrate, we observed a decrease in its mRNA binding. This could have resulted from other factors (RBPs or small RNAs) that can bind to the 3'UTR and outcompete HuR in the presence of butyrate. Indeed, we have observed alterations in the expression of many different RBPs in the presence of butyrate (Fig. 1A). Young et al. have shown that miR-16 and HuR, with antagonistic effects on COX-2 expression, compete for binding to its 3'UTR [57]. Moreover, an activated p38/MK2 axis was shown to enhance the binding of HuR to the 3'UTR of TNFα through phosphorylation and inhibition of binding of the competing destabilizing protein TTP [43]. Therefore, it is likely that reduced p38 activation in the presence of butyrate in the current study resulted in both reduced cytoplasmic translocation (as seen in HT-29 cells) and reduced target mRNA binding (as seen in Caco-2 cells) of HuR. Tong et al. [58] reported the lack of any inhibition of p38 phosphorylation in HT-29 cells treated with butyrate. However, in that study (unlike the current study), the cells were stimulated with TNFα, which itself is known to strongly enhance the phosphorylation of p38 [59]. Therefore, it is likely that in TNFα stimulated cells, the phosphorylation of p38 was via a signaling pathway that could not be inhibited in the presence of butyrate.

Phosphorylation of HuR at S88, S100 and T118 through the cell cycle related kinase Chk2 can also enhance the nuclear retention of HuR in a cell cycle dependent manner, especially at the S/G2 transition [45]. We observed that when synchronized and subsequently released HT-29 cells were treated with butyrate, the proportion of cells at the S and G2 phases increased in a temporal manner, which was accompanied by a remarkable increase in the phosphorylation of Chk2, and a reduction in the cytosolic levels of HuR. Interestingly, we did not observe any changes in the phosphorylation of Chk2 in Caco-2 cells, which also corroborates with a lack of change in cytosolic translocation of HuR observed in these cells (Fig. 2D).

Reporter gene assays showed that several different sequences could be stabilized when HuR was overexpressed; however, in the presence of butyrate, this stabilization function was lost with a reduction in the reporter signal. The fact that overexpression of HuR could not reverse the inhibitory effect of NaBt on reporter activity can be evaluated in two ways. First, other RBPs (such as TTP [18]) could outcompete the binding of HuR to mRNA sequences in the presence of NaBt and were functional in suppressing reporter activity. Second, signaling pathways activated in the presence of NaBt that reduce the cytosolic translocation or mRNA binding of HuR may persist even when HuR is available in supra-physiological amounts. It is known that overexpressed HuR localizes to the nucleus [60]; therefore, butyrate mediated inhibition in p38/MAPK signaling or increase in Chk2 signaling could have inhibited the cytosolic localization or mRNA binding of HuR even in HuR overexpressing cells.

Butyrate treatment has been shown to reduce the expression of several inflammatory cytokines such as IL-8, IL-17, IL-1b, IL-6, IL-12 and TNF-α in colonic epithelial cells through the inhibition of transcription factors such as NF-κB [61,62]. In the current study we did not observe any remarkable or consistent reduction in the transcriptional activation of NF-κB in the presence of butyrate in the cell line models we used, and therefore hypothesized that the anti-inflammatory function of butyrate could also be attributed, at least in part, to the destabilization of inflammatory mRNAs. We chose COX-2 as a candidate gene as it is already known to be extensively regulated in a post-transcriptional manner, and is known to be transcriptionally upregulated by NF-κB [63]. In fact, butyrate and other HDAC inhibitors such as Trichostatin A (TSA) and SAHA were shown to enhance the transcriptional activity of Early Growth Response protein 1 (EGR1) and thereby the expression of the destabilizing protein TTP resulting in the destabilization of COX-2 mRNA [18]. Indeed, the expression of TTP (*Zpf36*) was observed to be increased very early in our in silico analysis of mouse colonic epithelial cells treated with butyrate (Supplementary Fig. 1B).

We observed that the mRNA levels of COX-2 were considerably lower in the presence of butyrate even when new mRNA synthesis was blocked with Actinomycin D. Moreover, the enhanced stability of COX-2 mediated through the binding of overexpressed HuR to the 3'UTR of COX-2 could be reversed in the presence of butyrate. Additionally, using RNA IP, we observed that the binding of endogenous HuR to the 3'UTR of COX-2 was reduced in butyrate treated cells. Overall, our data indicate that NaBt treatment resulted in the reduced cytoplasmic translocation of HuR which could then lead to a reduction in the mRNA stability of COX-2.

Inflammation is essential to protect the host organism from infection and other insults. When an inflammatory response occurs, it is normally well-regulated with several mechanisms in place for self-limitation and rapid resolution [64]. Self-regulation can include many processes such as secretion of anti-inflammatory cytokines, inhibition of pro-inflammatory signal cascades, removal of receptors for inflammatory mediators, and activation of regulatory cells. Two studies carried out on animals fed with a fiber enriched diet showed increased production of butyrate in the colon and higher levels of butyrate in the feces. In both studies reduction in inflammatory signaling was reported [65,66]. It has also been suggested that the benefits of dietary supplementation of butyrate through a high fiber diet are more apparent at the tissue level in the colon rather than in the systemic circulation [8], indicating therapeutic opportunities for the gut epithelium. Our data suggest that in addition to the well-known effects of butyrate in reducing the activation of NF-κB and transcription of pro-inflammatory cytokines, the SCFA may also regulate the stability of inflammatory mRNAs at the post-transcriptional level through the regulation in expression and cytosolic translocation of RNA binding proteins.

It should be pointed out that the beneficial effects of the SCFA propionate has been questioned recently whereby the metabolite was shown to increase hyperglycemia and weight gain by increasing glycogenolysis and release of glucagon [67]. Additionally, low dose (0.05 mM) treatment of butyrate (but not propionate or acetate) was shown to enhance proliferation and fibrosis in hepatocytes in vitro; long term dietary consumption of butyrate (100 mM) in mice led to increased hepatic inflammation, fibrosis and expression of hepatocellular

carcinoma markers, although no tumors were seen [68]. In the current study we focused on HuR; however, the expression and cytoplasmic translocation of several other RBPs were also reduced in the presence of butyrate. It remains to be seen which mRNAs these RBPs target and what biological effect such targeting may have. Future studies are needed to better elucidate the precise role of microbial derived SCFAs on gene expression and metabolism, particularly in the context of gastrointestinal cancers.

Supplementary data to this article can be found online at https://doi.org/10.1016/j.cellsig.2019.109410.

Acknowledgements

This study was supported by the TUBITAK grant 215Z107 to SB. Partial support was obtained from Bilecik Şeyh Edebali University, Scientific Research Fund (Project no: 2018-01.BŞEÜ.12-01) to ST. The authors gratefully acknowledge Dr. Khalid S. A. Khabar for generously sharing the constructs. Ayşe Güniz Sirt is acknowledged for technical assistance. Members of the Banerjee Lab are acknowledged for many helpful discussions. Drs Mesut Muyan, Elif Erson and Mayda Gursel of METU are gratefully acknowledged for sharing reagents and protocols.

Author contributions: AT, SE, IS, ST and DHU carried out the experiments. SB supervised the study and wrote the paper.

References

[1] A. Rivière, M. Selak, D. Lantin, F. Leroy, L. De Vuyst, Bifidobacteria and butyrate-producing colon bacteria: importance and strategies for their stimulation in the human gut, Front. Microbiol. (2016), https://doi.org/10.3389/fmicb.2016.00979.
[2] S.E. Pryde, S.H. Duncan, G.L. Hold, C.S. Stewart, H.J. Flint, The microbiology of butyrate formation in the human colon, FEMS Microbiol. Lett. (2002), https://doi.org/10.1016/S0378-1097(02)01106-0.
[3] R.B. Canani, M. Di Costanzo, L. Leone, M. Pedata, R. Meli, A. Calignano, Potential beneficial effects of butyrate in intestinal and extraintestinal diseases, World J. Gastroenterol. (2011), https://doi.org/10.3748/wjg.v17.i12.1519.
[4] N. Wu, X. Yang, R. Zhang, J. Li, X. Xiao, Y. Hu, Y. Chen, F. Yang, N. Lu, Z. Wang, C. Luan, Y. Liu, B. Wang, C. Xiang, Y. Wang, F. Zhao, G.F. Gao, S. Wang, L. Li, H. Zhang, B. Zhu, Dysbiosis signature of fecal microbiota in colorectal Cancer patients, Microb. Ecol. (2013), https://doi.org/10.1007/s00248-013-0245-9.
[5] R. Berni Canani, M. Di Costanzo, L. Leone, The epigenetic effects of butyrate: potential therapeutic implications for clinical practice, Clin. Epigenetics (2012), https://doi.org/10.1186/1868-7083-4-4.
[6] S.M. McNabney, T.M. Henagan, Short chain fatty acids in the colon and peripheral tissues: a focus on butyrate, colon cancer, obesity and insulin resistance, Nutrients. (2017), https://doi.org/10.3390/nu9121348.
[7] P. Sossai, Butyric acid: what is the future for this old substance? Swiss Med. Wkly. (2012), https://doi.org/10.4414/smw.2012.13596.
[8] M.C.P. Cleophas, J.M. Ratter, S. Bekkering, J. Quintin, K. Schraa, E.S. Stroes, M.G. Netea, L.A.B. Joosten, Effects of oral butyrate supplementation on inflammatory potential of circulating peripheral blood mononuclear cells in healthy and obese males, Sci. Rep. (2019), https://doi.org/10.1038/s41598-018-37246-7.
[9] P. Kafasla, A. Skliris, D.L. Kontoyiannis, Post-transcriptional coordination of immunological responses by RNA-binding proteins, Nat. Immunol. (2014), https://doi.org/10.1038/ni.2884.
[10] K.S.A. Khabar, Post-transcriptional control during chronic inflammation and cancer: a focus on AU-rich elements, Cell. Mol. Life Sci. (2010), https://doi.org/10.1007/s00018-010-0383-x.
[11] S.J. Cok, S.J. Acton, A.R. Morrison, The proximal region of the 3′-untranslated region of cyclooxygenase-2 is recognized by a multimeric protein complex containing HuR, TIA-1, TIAR, and the heterogeneous nuclear ribonucleoprotein U, J. Biol. Chem. 278 (2003) 36157–36162, https://doi.org/10.1074/jbc.M302547200.
[12] T. MINO, O. TAKEUCHI, Post-transcriptional regulation of immune responses by RNA binding proteins, Proc. Jpn. Acad. Ser. B. 94 (2018) 248–258, https://doi.org/10.2183/pjab.94.017.
[13] K. Masuda, Y. Kuwano, Diverse roles of RNA-binding proteins in cancer traits and their implications in gastrointestinal cancers, Wiley Interdiscip. Rev. RNA. 1 (2018) e1520, , https://doi.org/10.1002/wrna.1520.
[14] K. Masuda, Y. Kuwano, K. Nishida, K. Rokutan, General RBP expression in human tissues as a function of age, Ageing Res. Rev. (2012), https://doi.org/10.1016/j.arr.2012.01.005.
[15] A. Doller, J. Pfeilschifter, W. Eberhardt, Signalling pathways regulating nucleo-cytoplasmic shuttling of the mRNA-binding protein HuR, Cell. Signal. (2008), https://doi.org/10.1016/j.cellsig.2008.05.007.
[16] H.K. Hyeon, M. Gorospe, Phosphorylated HuR Shuttles in cycles, Cell Cycle (2008), https://doi.org/10.4161/cc.7.20.6884.
[17] S. Lebedeva, M. Jens, K. Theil, B. Schwanhäusser, M. Selbach, M. Landthaler, N. Rajewsky, Transcriptome-wide analysis of regulatory interactions of the RNA-binding protein HuR, Mol. Cell (2011), https://doi.org/10.1016/j.molcel.2011.06.008.
[18] C. Sobolewski, S. Sanduja, F.F. Blanco, L. Hu, D.A. Dixon, Histone deacetylase inhibitors activate tristetraprolin expression through induction of early growth response protein 1 (EGR1) in colorectal cancer cells, Biomolecules (2015), https://doi.org/10.3390/biom5032035.
[19] X.T. Zheng, X.Q. Xiao, Sodium butyrate down-regulates tristetraprolin-mediated cyclin B1 expression independent of the formation of processing bodies, Int. J. Biochem. Cell Biol. 69 (2015) 241–248, https://doi.org/10.1016/j.biocel.2015.11.002.
[20] J. Fukae, Y. Amasaki, Y. Yamashita, T. Bohgaki, S. Yasuda, S. Jodo, T. Atsumi, T. Koike, Butyrate suppresses tumor necrosis factor α production by regulating specific messenger RNA degradation mediated through a cis-acting AU-rich element, Arthritis Rheum. 52 (2005) 2697–2707, https://doi.org/10.1002/art.21258.
[21] T. Bakheet, ARED: human AU-rich element-containing mRNA database reveals an unexpectedly diverse functional repertoire of encoded proteins, Nucleic Acids Res. 29 (2001) 246–254, https://doi.org/10.1093/nar/29.1.246.
[22] K.A. Harper, A.J. Tyson-Capper, Complexity of COX-2 gene regulation, Biochem. Soc. Trans. 36 (2008) 543–545, https://doi.org/10.1042/BST0360543.
[23] P. Sarker, Expression Data from HT-29, a Human Colonic Epithelial Cell Line, n.d https://www.ncbi.nlm.nih.gov/geo/query/acc.cgi?acc=GSE45220 accessed July 16, 2019.
[24] Y. Tabuchi, I. Takasaki, T. Doi, Y. Ishii, H. Sakai, T. Kondo, Genetic networks responsive to sodium butyrate in colonic epithelial cells, FEBS Lett. 580 (2006) 3035–3041, https://doi.org/10.1016/j.febslet.2006.04.048.
[25] J. Hnilicová, S. Hozeifi, E. Dušková, J. Icha, T. Tománková, D. Staněk, Histone deacetylase activity modulates alternative splicing, PLoS One (2011), https://doi.org/10.1371/journal.pone.0016727.
[26] A. Wullaert, M.C. Bonnet, M. Pasparakis, NF-κB in the regulation of epithelial homeostasis and inflammation, Cell Res. 21 (2011) 146–158, https://doi.org/10.1038/cr.2010.175.
[27] R.A. Irizarry, B.M. Bolstad, F. Collin, L.M. Cope, B. Hobbs, T.P. Speed, Summaries of affymetrix genechip probe level data, Nucleic Acids Res (2003), https://doi.org/10.1093/nar/gng015.
[28] B.S. Carvalho, R.A. Irizarry, A framework for oligonucleotide microarray preprocessing, Bioinformatics (2010), https://doi.org/10.1093/bioinformatics/btq431.
[29] K.B. Cook, H. Kazan, K. Zuberi, Q. Morris, T.R. Hughes, RBPDB: A database of RNA-binding specificities, Nucleic Acids Res. (2011), https://doi.org/10.1093/nar/gkq1069.
[30] J.W. MacDonald, hugene10sttranscriptcluster.db: Affymetrix hugene10 annotation data (chip hugene10sttranscriptcluster), (2017).
[31] J.W. MacDonald, huex10sttranscriptcluster.db: Affymetrix huex10 annotation data (chip huex10sttranscriptcluster), (2017).
[32] M.E. Ritchie, B. Phipson, D. Wu, Y. Hu, C.W. Law, W. Shi, G.K. Smyth, Limma powers differential expression analyses for RNA-sequencing and microarray studies, Nucleic Acids Res 43 (2015) e47, https://doi.org/10.1093/nar/gkv007.
[33] P. Shannon, A. Markiel, O. Ozier, N.S. Baliga, J.T. Wang, D. Ramage, N. Amin, B. Schwikowski, T. Ideker, Cytoscape: a software environment for integrated models of biomolecular interaction networks, Genome Res. 13 (2003) 2498–2504, https://doi.org/10.1101/gr.1239303.
[34] L. Young, J. Sung, J.R. Masters, Detection of mycoplasma in cell cultures, Nat. Protoc. (2010), https://doi.org/10.1038/nprot.2010.43.
[35] S. Tunçer, S. Banerjee, Determination of autophagy in the caco-2 spontaneously differentiating model of intestinal epithelial cells, Methods Mol. Biol. (2019), https://doi.org/10.1007/7651_2017_66.
[36] M.W. Pfaffl, A new mathematical model for relative quantification in real-time RT-PCR, Nucleic Acids Res. 29 (2001) e45, , https://doi.org/10.1093/nar/29.9.e45.
[37] S.A. Bustin, V. Benes, J.A. Garson, J. Hellemans, J. Huggett, M. Kubista, R. Mueller, T. Nolan, M.W. Pfaffl, G.L. Shipley, J. Vandesompele, C.T. Wittwer, The MIQE guidelines: minimum information for publication of quantitative real-time PCR experiments, Clin. Chem. 55 (2009) 611–622, https://doi.org/10.1373/clinchem.2008.112797.
[38] E. Hitti, S. Al-Yahya, M. Al-Saif, P. Mohideen, L. Mahmoud, S.J.S.J. Polyak, K.S.A. Khabar, A versatile ribosomal protein promoter-based reporter system for selective assessment of RNA stability and post-transcriptional control, RNA 16 (2010) 1245–1255, https://doi.org/10.1261/rna.2026310.
[39] T. Peritz, F. Zeng, T.J. Kannanayakal, K. Kilk, E. Eiríksdóttir, U. Langel, J. Eberwine, Immunoprecipitation of mRNA-protein complexes, Nat. Protoc. 1 (2006) 577–580, https://doi.org/10.1038/nprot.2006.82.
[40] I. Topisirovic, N. Siddiqui, S. Orolicki, L. Skrabanek, M. Tremblay, T. Hoang, K. Borden, Stability of eukaryotic translation initiation factor 4E mRNA is regulated by HuR, and this activity is dysregulated in cancer, Mol. Cell. Biol. (2009), https://doi.org/10.1128/MCB.01532-08.
[41] S. Helfer, J. Schott, G. Stoecklin, K. Förstemann, AU-rich element-mediated mRNA decay can occur independently of the miRNA Machinery in mouse embryonic fibroblasts and drosophila S2-cells, PLoS One (2012), https://doi.org/10.1371/journal.pone.0028907.
[42] L. Munoz, B. Heng, T. Grewal, J. Haapasalo, F.M.S. Gurgis, A.J. Ammit, M.X.M. Tang, Y.T. Yeung, H. Haapasalo, M. Buckland, G.J. Guillemin, The p38-MK2-HuR pathway potentiates EGFRvIII–IL-1β-driven IL-6 secretion in glioblastoma cells, Oncogene. 34 (2014) 2934–2942, https://doi.org/10.1038/onc.2014.225.
[43] C. Tiedje, N. Ronkina, M. Tehrani, S. Dhamija, K. Laass, H. Holtmann, A. Kotlyarov, M. Gaestel, The p38/MK2-driven exchange between tristetraprolin and HuR regulates AU-rich element-dependent translation, PLoS Genet. (2012), https://doi.org/10.1371/journal.pgen.1002977.

[44] H.H. Kim, K. Abdelmohsen, M. Gorospe, Regulation of HuR by DNA damage response kinases, J. Nucleic Acids. (2010), https://doi.org/10.4061/2010/981487.
[45] K. Abdelmohsen, R. Pullmann, A. Lal, H.H. Kim, S. Galban, X. Yang, J.D. Blethrow, M. Walker, J. Shubert, D.A. Gillespie, H. Furneaux, M. Gorospe, Phosphorylation of HuR by Chk2 regulates SIRT1 expression, Mol. Cell (2007), https://doi.org/10.1016/j.molcel.2007.01.011.
[46] Y.D.P. Limasale, A. Tezcaner, C. Özen, D. Keskin, S. Banerjee, Epidermal growth factor receptor-targeted immunoliposomes for delivery of celecoxib to cancer cells, Int. J. Pharm. 479 (2015) 364–373, https://doi.org/10.1016/j.ijpharm.2015.01.016.
[47] I. Russo, A. Luciani, P. De Cicco, E. Troncone, C. Ciacci, Butyrate attenuates lipopolysaccharide-induced inflammation in intestinal cells and Crohn's mucosa through modulation of antioxidant defense machinery, PLoS One 7 (2012), https://doi.org/10.1371/journal.pone.0032841 e32841.
[48] O. Bensaude, Inhibiting eukaryotic transcription: which compound to choose? how to evaluate its activity? Transcription (2011), https://doi.org/10.4161/trns.2.3.16172.
[49] S. Siavoshian, J.P. Segain, M. Kornprobst, C. Bonnet, C. Cherbut, J.P. Galmiche, H.M. Blottière, Butyrate and trichostatin a effects on the proliferation/differentiation of human intestinal epithelial cells: induction of cyclin D3 and p21 expression, Gut (2000), https://doi.org/10.1136/gut.46.4.507.
[50] E. Astarci, A. Sade, I. Cimen, B. Savaş, S. Banerjee, The NF-κB target genes ICAM-1 and VCAM-1 are differentially regulated during spontaneous differentiation of Caco-2 cells, FEBS J. 279 (2012) 2966–2986, https://doi.org/10.1111/j.1742-4658.2012.08677.x.
[51] D.L. Topping, P.M. Clifton, Short-chain fatty acids and human colonic function: roles of resistant starch and nonstarch polysaccharides, Physiol. Rev. 81 (2001) 1031–1064, https://doi.org/10.1152/physrev.2001.81.3.1031.
[52] J.H. Cummings, E.W. Pomare, H.W.J. Branch, C.P.E. Naylor, G.T. MacFarlane, Short chain fatty acids in human large intestine, portal, hepatic and venous blood, Gut (1987), https://doi.org/10.1136/gut.28.10.1221.
[53] J.M. Mariadason, HDACs and HDAC inhibitors in colon cancer., Epigenetics. 3, 28–37. doi:10.4161/epi.3.1.5736
[54] M. Krishnan, A.B. Singh, J.J. Smith, A. Sharma, X. Chen, S. Eschrich, T.J. Yeatman, R.D. Beauchamp, P. Dhawan, HDAC inhibitors regulate claudin-1 expression in colon cancer cells through modulation of mRNA stability, Oncogene. 29 (2010) 305–312, https://doi.org/10.1038/onc.2009.324.
[55] K. Abdelmohsen, M. Gorospe, Posttranscriptional regulation of cancer traits by HuR, Wiley Interdiscip. Rev. RNA. 1 (2010) 214–229, https://doi.org/10.1002/wrna.4.
[56] R. Winzen, M. Kracht, B. Ritter, A. Wilhelm, C.Y.A. Chen, A. Bin Shyu, M. Müller, M. Gaestel, K. Resch, H. Holtmann, The p38 MAP kinase pathway signals for cytokine-induced mrna stabilization via map kinase-activated protein kinase 2 and an AU-rich region-targeted mechanism, EMBO J. (1999), https://doi.org/10.1093/emboj/18.18.4969.
[57] L.E. Young, A.E. Moore, L. Sokol, N. Meisner-Kober, D.A. Dixon, The mRNA stability factor HuR inhibits microRNA-16 targeting of COX-2, Mol. Cancer Res. 10 (2012) 167–180, https://doi.org/10.1158/1541-7786.MCR-11-0337.
[58] X. Tong, L. Yin, C. Giardina, Butyrate suppresses cox-2 activation in colon cancer cells through HDAC inhibition, Biochem. Biophys. Res. Commun. 317 (2004) 463–471, https://doi.org/10.1016/j.bbrc.2004.03.066.
[59] B.B. Aggarwal, S. Shishodia, Y. Takada, D. Jackson-Bernitsas, K.S. Ahn, G. Sethi, H. Ichikawa, TNF blockade: an inflammatory issue, Cytokines as Potential Ther. Targets Inflamm. Ski. Dis, 2006, https://doi.org/10.1007/3-540-37673-9_10.
[60] X.C. Fan, J.A. Steitz, Overexpression of HuR, a nuclear-cytoplasmic shuttling protein, increases the in vivo stability of ARE-containing mRNAs, EMBO J. (1998), https://doi.org/10.1093/emboj/17.12.3448.
[61] M.H. Kim, S.G. Kang, J.H. Park, M. Yanagisawa, C.H. Kim, Short-chain fatty acids activate GPR41 and GPR43 on intestinal epithelial cells to promote inflammatory responses in mice, Gastroenterology (2013), https://doi.org/10.1053/j.gastro.2013.04.056.
[62] J.P. Segain, J.P. Galmiche, D. Raingeard De La Blétière, A. Bourreille, V. Leray, N. Gervois, C. Rosales, L. Ferrier, C. Bonnet, H.M. Blottière, Butyrate inhibits inflammatory responses through NFκB inhibition: implications for Crohn's disease, Gut (2000), https://doi.org/10.1136/gut.47.3.397.
[63] K.A. Harper, A.J. Tyson-Capper, Complexity of COX - 2 gene regulation, Biochem. Soc. Trans. 36 (2008) 543–545, https://doi.org/10.1042/BST0360543.
[64] K.E.B. Knudsen, H.N. Lærke, M.S. Hedemann, T.S. Nielsen, A.K. Ingerslev, D.S.G. Nielsen, P.K. Theil, S. Purup, S. Hald, A.G. Schioldan, M.L. Marco, S. Gregersen, K. Hermansen, Impact of diet-modulated butyrate production on intestinal barrier function and inflammation, Nutrients (2018), https://doi.org/10.3390/nu10101499.
[65] E. Hijová, V. Szabadosova, J. Štofilová, G. Hrčková, Chemopreventive and metabolic effects of inulin on colon cancer development, J. Vet. Sci. (2013), https://doi.org/10.4142/jvs.2013.14.4.387.
[66] M.E. Rodríguez-Cabezas, J. Gálvez, M.D. Lorente, A. Concha, D. Camuesco, S. Azzouz, A. Osuna, L. Redondo, A. Zarzuelo, Dietary fiber Down-regulates colonic tumor necrosis factor α and nitric oxide production in Trinitrobenzenesulfonic acid-induced Colitic rats, J. Nutr. (2018), https://doi.org/10.1093/jn/132.11.3263.
[67] A. Tirosh, E.S. Calay, G. Tuncman, K.C. Claiborn, K.E. Inouye, K. Eguchi, M. Alcala, M. Rathaus, K.S. Hollander, I. Ron, R. Livne, Y. Heianza, L. Qi, I. Shai, R. Garg, G.S. Hotamisligil, The short-chain fatty acid propionate increases glucagon and FABP4 production, impairing insulin action in mice and humans, Sci. Transl. Med. (2019), https://doi.org/10.1126/scitranslmed.aav0120.
[68] V. Singh, B.S. Yeoh, B. Chassaing, X. Xiao, P. Saha, R. Aguilera Olvera, J.D. Lapek, L. Zhang, W.B. Wang, S. Hao, M.D. Flythe, D.J. Gonzalez, P.D. Cani, J.R. Conejo-Garcia, N. Xiong, M.J. Kennett, B. Joe, A.D. Patterson, A.T. Gewirtz, M. Vijay-Kumar, Dysregulated microbial fermentation of soluble fiber induces cholestatic liver cancer, Cell (2018), https://doi.org/10.1016/j.cell.2018.09.004.